J. Fluid Mech. (1992), *vol.* 242, *pp.* 349–370
Printed in Great Britain

Rapid distortion theory for homogeneous compressed turbulence with application to modelling

By P. A. DURBIN AND O. ZEMAN
Center for Turbulence Research, Stanford University, Stanford, CA 94035-3030, USA

(Received 26 September 1991 and in revised form 19 February 1992)

Compressible rapid distortion theory is used to examine pressure fluctuations and the pressure–dilatation correlation in a field of turbulence subjected to rapid homogeneous compression. It is shown how a one-dimensional compression produces large solenoidal pressure fluctuations. As the dimensionality of the compression increases, the magnitude of these fluctuations decreases – it vanishes for a spherically symmetric compression. By contrast the dilatational, or acoustic, pressure fluctuations depend mainly on the net volumetric compression, and are relatively insensitive to the dimensionality of the compression. These same comments apply to the pressure–dilatation correlation.

The pressure–dilatation correlation appears in the compressible turbulent kinetic energy equation and is significant in rapidly evolving flows; Reynolds stress closure models require that it be represented. The continuity equation provides a relation between pressure dilatation and the rate of change of pressure fluctuation variance. This relation is the basis for our RDT analysis. That analysis leads to a proposal for modelling the rapid contribution to pressure dilatation.

1. Introduction

Rapid distortion theory (RDT) provides a means for examining processes which occur in turbulent flows when the timescale of the rate of distortion of turbulence is much shorter than the characteristic timescale of the large eddies. In the present paper we solve the irrotational, compressible RDT equations to determine the pressure variance and the pressure–dilatation correlation in homogeneously compressed turbulence at small fluctuating Mach numbers. Zeman (1991) observed that in direct numerical simulations (Coleman & Mansour 1991) of rapid one-dimensional compression of nearly incompressible, homogeneous turbulence, the pressure–dilatation term in the turbulent kinetic energy acts as a significant sink of energy; it can be an order of magnitude larger than the dissipation term, and therefore must be represented in turbulence models which deal with flows containing one- or two-dimensional compressions. Such flows include turbulence/shock wave interactions, the compression corner and the compression stroke of an internal combustion engine (Wong & Hoult 1979). These are cases in which turbulence may indeed be subjected to rapid distortion.

It is evident from direct numerical simulations (DNS) of turbulence passing through a shock (Lee, Lele & Moin 1991), that the pressure–dilatation correlation plays an important role in the turbulence energy balance in the vicinity of the shock.

The pressure dilatation converts kinetic energy to 'potential' energy during compression and then partially restores it after the compression.

Coleman & Mansour (1991) found by DNS that the Spiegel–Frisch transformation between low-Mach-number spherically compressed turbulence and decaying isotropic turbulence provides a basis for understanding spherically compressed turbulence. But, the existence of this transformation into isotropic decay also suggests that spherical compression will not reveal the essential effects of compression upon turbulent flow. In the applications cited above, the compression is not spherically symmetric. DNS of unsymmetric compressions show some striking effects of asymmetry (Zeman 1991). Of present interest is the observation that the ratio of pressure–dilatation correlation to dissipation rate is enormously greater for a one-dimensional compression than for a spherical compression. The present analysis provides a simple explanation for that difference: the rapid, solenoidal pressure vanishes for spherical compression, but becomes quite large for a one-dimensional compression. The larger pressure dilatation causes a pronounced reduction in turbulent kinetic energy. Another noteworthy result of the DNS is that, at the low turbulence Mach numbers of present interest, the pressure variance grows far more rapidly in one-dimensional than in spherical compression; again, the present linear analysis is consistent with this result.

A Reynolds stress analysis for the case to be addressed in this paper, essentially, was given by Batchelor & Proudman (1954) and Ribner & Tucker (1953): Batchelor & Proudman considered incompressible flow, while Ribner & Tucker examined the distortion of solenoidal turbulence by a compressible mean flow. The Reynolds stress analysis will not be repeated here, nor will the formal justifications of the rapid distortion approximation, which have been explained at length in reviews such as that by Hunt & Carruthers (1990). It suffices to say that RDT uses linearized, inviscid equations, combined with statistical averaging, to describe the evolution of a field of turbulence in response to strong distortions by the mean flow. A previous application of RDT to pressure fluctuations, although for incompressible flow, is described in Durbin & Hunt (1980).

Batchelor & Proudman (1954) and Ribner & Tucker (1953) provided solutions for homogeneously distorted turbulence. Their solutions for strictly homogeneous turbulence also provide a quasi-homogeneous (or small-scale) approximation to non-homogeneously distorted turbulence, provided that entropy fluctuations can be neglected. The non-homogeneous compressible RDT of Goldstein (1978) allows for vorticity generation by entropy fluctuations, but this effect cannot occur in the strictly homogeneous case; Goldstein (1979) examined the production of turbulence from entropy fluctuations. In the incompressible RDT, a transformation can be introduced to relate the strictly homogeneous solutions to the quasi-homogeneous approximation, without symmetry restrictions (Durbin 1981). In the present compressible theory, quasi-homogeneity also requires a high-frequency approximation for the acoustic mode. The analysis in the following text is for the strictly homogeneous distortion; the quasi-homogeneous case is considered in Appendix A.

Because of the approximations and idealizations made, the RDT solution is of limited predictive value – of course, it does describe quite well situations where the approximations are satisfied. Some level of Reynolds stress closure is normally used for practical computations of turbulent flow. Rapid distortion analysis gives guidance to the development of such models: in the present paper we propose a rapid pressure dilatation model. The model provides excellent agreement with DNS data. Zeman (1991) previously proposed an algebraic model to account for the large rapid contribution to pressure dilatation in one-dimensional, and its absence in three-dimensional, spherical compression. That model yields correct magnitudes of pressure dilatation, but the pointwise agreement with data is less satisfactory than the present model, in part because Zeman's is an algebraic model.

2. Mean flow

The requirement for homogeneity in compressible flow is more stringent than in incompressible flow. In the former case both the mean flow gradients and mean pressure must be spatially uniform; in the latter the mean pressure need not be uniform. The requirement of uniform velocity gradient means that U has the form $U = x \cdot \boldsymbol{S}(t)$; the requirement of uniform pressure, substituted into the inviscid momentum equation, shows that the velocity satisfies $\mathrm{D}U/\mathrm{D}t = 0$, and hence that $\boldsymbol{S}$ must satisfy

$$\dot{\boldsymbol{S}} + \boldsymbol{S} \cdot \boldsymbol{S} = 0. \tag{1}$$

The dot denotes differentiation with respect to time. In the present case of irrotational mean flow, the solution to (1) is

$$\boldsymbol{S} = \begin{pmatrix} a_1/(1+a_1 t) & 0 & 0 \\ 0 & a_2/(1+a_2 t) & 0 \\ 0 & 0 & a_3/(1+a_3 t) \end{pmatrix} \tag{2}$$

in which the a_i are constants. Although this is the only time-dependence consistent with homogeneity, it actually represents a fairly general distorting strain because the a_i are arbitrary. $\boldsymbol{S}$ is the rate of strain matrix. To facilitate the RDT solution we introduce the matrix

$$\boldsymbol{J} = \begin{pmatrix} 1/(1+a_1 t) & 0 & 0 \\ 0 & 1/(1+a_2 t) & 0 \\ 0 & 0 & 1/(1+a_3 t) \end{pmatrix}. \tag{3}$$

Note that $\boldsymbol{S} = \boldsymbol{S}(0) \cdot \boldsymbol{J}$ and that $\boldsymbol{J}$ satisfies

$$\dot{\boldsymbol{J}} + \boldsymbol{S} \cdot \boldsymbol{J} = 0. \tag{4}$$

If the mean vorticity were not zero $\boldsymbol{J}$ would contain off-diagonal terms, and would not be symmetric. That asymmetry greatly complicates the RDT theory for mean shear flows. $\boldsymbol{J}$ is the transformation from Lagrangian to Eulerian coordinates that arises in classical RDT analysis (Batchelor & Proudman 1954).

The mean density, as determined by continuity, and the adiabatic sound speed are given by

$$\rho = \rho_0 \operatorname{Det}(\boldsymbol{J}); \quad c^2 = c_0^2[\operatorname{Det}(\boldsymbol{J})]^{\gamma-1}$$

where, as usual γ is the ratio of specific heats. In the present case of rapid, homogeneous compression, dissipative heating is not important. Pressure and density are related by the isentropic formula $P/\rho^\gamma = \text{constant}$.

3. Fluctuations

Given that ρ is spatially uniform, and that $\mathrm{D}U/\mathrm{D}t = 0$ and $\mathrm{D}\rho/\mathrm{D}t = -\rho \nabla \cdot U$, the linearized, inviscid fluctuating momentum, continuity and entropy equations are

$$\left.\begin{aligned} \rho(\mathrm{D}\boldsymbol{u}'/\mathrm{D}t + \boldsymbol{u}' \cdot \nabla U) &= -\nabla p', \\ \mathrm{D}(\rho'/\rho)/\mathrm{D}t &= -\nabla \cdot \boldsymbol{u}', \\ \mathrm{D}s'/\mathrm{D}t &= 0. \end{aligned}\right\} \tag{5}$$

There are the equations used in RDT. In (5) s' is the fluctuating entropy; $\mathrm{D}/\mathrm{D}t$ is the convective derivative following the mean flow, $\partial_t + \boldsymbol{U}\cdot\boldsymbol{\nabla}$; primes denote fluctuating variables; and unprimed variables represent mean values. The conservation of entropy implies that $\gamma\mathrm{D}(\rho'/\rho)/\mathrm{D}t = \mathrm{D}(p'/P)/\mathrm{D}t$, so the continuity equation can be replaced by

$$\mathrm{D}(p'/\gamma P)/\mathrm{D}t = -\boldsymbol{\nabla}\cdot\boldsymbol{u}'. \tag{6}$$

For future reference, we note that (6) enables the pressure–dilatation correlation to be computed from the pressure variance:

$$\overline{p'\nabla\cdot\boldsymbol{u}'} = -\tfrac{1}{2}\gamma P\frac{\mathrm{d}}{\mathrm{d}t}\left(\frac{\overline{p'^2}}{(\gamma P)^2}\right). \tag{7}$$

The overbar denotes ensemble averaging. Our primary results, and our new developments on closure modelling, derive from (7). The momentum equation and (6) form a closed system for $\boldsymbol{u}'$ and p'. The requirement of homogeneity of the mean pressure prevents entropy fluctuations from generating turbulent velocity fluctuations. Turbulent velocity generation by entropy fluctuations is a phenomenon which non-homogeneous RDT is able to describe (Goldstein 1978, 1979).

To obtain a solution to the governing linearized equations, we introduce a Fourier representation of the initial field. Then the RDT analysis can be performed by solving for each wavenumber component separately (Hunt 1973; Hunt & Carruthers 1990). Thus, let

$$\boldsymbol{u}' = \int_{-\infty}^{\infty}\hat{\boldsymbol{u}}\,\mathrm{d}^3\boldsymbol{k}_0, \qquad p' = \int_{-\infty}^{\infty}\hat{p}\,\mathrm{d}^3\boldsymbol{k}_0. \tag{8}$$

A solution is sought in the form

$$\hat{\boldsymbol{u}} = \boldsymbol{A}(t)\,\mathrm{e}^{\mathrm{i}\boldsymbol{k}(t)\cdot\boldsymbol{x}}; \quad \hat{p} = B(t)\,\mathrm{e}^{\mathrm{i}\boldsymbol{k}(t)\cdot\boldsymbol{x}} \tag{9}$$

in which $\boldsymbol{k} = \boldsymbol{k}_0\cdot\boldsymbol{J}(t)$. Equation (4) and this formula for $\boldsymbol{k}$ indicate that $\mathrm{D}(\boldsymbol{k}\cdot\boldsymbol{x})/\mathrm{D}t = 0$. With (9), the governing equations (5) and (6) become

$$\rho(\dot{\boldsymbol{A}} + \boldsymbol{A}\cdot\boldsymbol{S}) = -\mathrm{i}\boldsymbol{k}B, \tag{10a}$$

$$\frac{\mathrm{d}(B/\gamma P)}{\mathrm{d}t} = -\mathrm{i}\boldsymbol{k}\cdot\boldsymbol{A}. \tag{10b}$$

Let

$$\boldsymbol{A} = \boldsymbol{\mathcal{A}} + \mathrm{i}\boldsymbol{k}\phi, \tag{11}$$

where $\boldsymbol{\mathcal{A}}(t) = \boldsymbol{\mathcal{A}}_0\cdot\boldsymbol{J}(t)$, with $\boldsymbol{\mathcal{A}}_0$ being a constant vector determined by the initial conditions. This decomposition of $\boldsymbol{A}$ is convenient because $\boldsymbol{\mathcal{A}}$ is a solution to (10a) with the right-hand side equated to zero. Hence, substituting (11) into (10a) gives

$$B = -\rho\dot{\phi} \tag{12}$$

and substituting this along with (11) into (10b) shows that ϕ satisfies

$$\frac{\mathrm{d}}{\mathrm{d}t}\left(c^{-2}\frac{\mathrm{d}\phi}{\mathrm{d}t}\right) + |\boldsymbol{k}|^2\phi = \mathrm{i}\boldsymbol{k}\cdot\boldsymbol{\mathcal{A}}. \tag{13}$$

Thus, the analysis reduces to solving the second-order ordinary differential equation (13) for ϕ – this formulation of compressible RDT was first presented by Goldstein (1978).

For a spherical compression $\boldsymbol{J} = \boldsymbol{I}/(1+at)$, where $\boldsymbol{I}$ is the identity matrix. Then (13) has the particular solution $\phi = \mathrm{i}\boldsymbol{k}\cdot\boldsymbol{\mathcal{A}}/|\boldsymbol{k}|^2$. If this is inserted into (11), one finds that the velocity is solenoidal (i.e. $\boldsymbol{k}\cdot\boldsymbol{A} = 0$). In addition to this particular solution, (13) will have a homogeneous solution, which is a dilatational, irrotational acoustic wave, uncoupled from the vortical, solenoidal component of the velocity (Sabelnikov 1975): the acoustic wave amplitude is determined entirely from the initial conditions; if the initial velocity is solenoidal then no acoustic component will exist and the turbulence will remain solenoidal for all time.

For general, non-spherical compressions, the vortical and acoustic modes will be coupled through the forcing term on the right-hand side of (13). If the time derivatives were absent from (13) its solution would be $\phi = \mathrm{i}\boldsymbol{k}\cdot\boldsymbol{\mathscr{A}}/|\boldsymbol{k}|^2$. Equation (13) can alternatively be formulated as an equation for the departure from this quasi-steady solution. Letting

$$\phi = \mathrm{i}\frac{\boldsymbol{k}\cdot\boldsymbol{\mathscr{A}}}{|\boldsymbol{k}|^2}+\phi_1 \tag{14}$$

(13) is replaced by
$$\frac{\mathrm{d}}{\mathrm{d}t}\left(c^{-2}\frac{\mathrm{d}\phi_1}{\mathrm{d}t}\right)+|\boldsymbol{k}|^2\phi_1 = -\mathrm{i}\frac{\mathrm{d}}{\mathrm{d}t}\left(c^{-2}\frac{\mathrm{d}}{\mathrm{d}t}\frac{\boldsymbol{k}\cdot\boldsymbol{\mathscr{A}}}{|\boldsymbol{k}|^2}\right). \tag{15}$$

The quantity being differentiated on the right-hand side of (15) evolves in time owing to distortion by the mean flow. This distortion occurs on the timescale $1/|a|$, where a represents one of the non-zero constants in (2). An acoustic wave generated by the temporal evolution of spatially homogeneous, vortical turbulence would have a wavelength equal to that of the distorted eddy. Hence, the acoustic frequency is of order c/L, where L is the integral scale of the turbulence. When the distortion timescale is long compared to the acoustic timescale, acoustic waves will not be generated efficiently. The forcing term in (15) will generate acoustic disturbances of amplitude $O(\Delta m)^2$, where $\Delta m = L|a|/c$. Δm is the change in mean flow Mach number across one integral scale of the turbulence (i.e. across one 'eddy'). In the quasi-homogeneous approximation – in which the eddy size must be small compared to the scale of mean flow variation – Δm^2 must be small (unless the mean flow Mach number is large compared to unity). Thus, the present analysis corresponds to the quasi-homogeneous limit only when the right-hand side of (15) is small; that is when the acoustic and vortical modes decouple to lowest order of approximation. We will invoke the small-Δm limit. It should be emphasized that even in this limit the pressure–dilatation correlation caused by vortical disturbances is not zero; it can be computed by the relation (7) – although strictly, this must be regarded as a higher-order effect of the lowest-order solenoidal field.

In the ensuing analysis, the velocity will be given by

$$\boldsymbol{A} = [\boldsymbol{\mathscr{A}}-\boldsymbol{k}(\boldsymbol{k}\cdot\boldsymbol{\mathscr{A}}/|\boldsymbol{k}|^2)]+\mathrm{i}\boldsymbol{k}\phi_1, \tag{16}$$

as follows from (11) and (14). The bracketed term in (16) is orthogonal to $\boldsymbol{k}$, and hence can be referred to as the solenoidal component of $\boldsymbol{A}$. Note that (16) is the Helmholtz decomposition of the velocity into solenoidal (the first two terms) and irrotational parts, while (11) is Goldstein's decomposition into vortical (but not solenoidal) and irrotational parts. It is clear from (16) that the two components of the Helmholtz decomposition of the velocity field are orthogonal when the turbulence is homogeneous. Other properties of the flow, such as the pressure fluctuations, are not decoupled by the Helmholtz decomposition. However, the present results will be obtained under the approximation that ϕ_1 is uncorrelated with the solenoidal part of (16).

4. Vortical mode

According to the preceding (see (12) and (14)), the vortical contribution to the pressure is given by

$$B = -\rho\dot{\phi} = -\mathrm{i}\rho\frac{\mathrm{d}}{\mathrm{d}t}\left(\frac{\boldsymbol{k}\cdot\mathscr{A}}{|\boldsymbol{k}|^2}\right)$$

$$= -\mathrm{i}\rho\frac{\mathrm{d}}{\mathrm{d}t}\left(\frac{\boldsymbol{k}_0\cdot\boldsymbol{J}^2\cdot\mathscr{A}_0}{\boldsymbol{k}_0\cdot\boldsymbol{J}^2\cdot\boldsymbol{k}_0}\right)$$

$$= -2\mathrm{i}\rho\left[\frac{\boldsymbol{k}_0\cdot\mathscr{S}\cdot\mathscr{A}_0}{|\boldsymbol{k}|^2} - (\boldsymbol{k}_0\cdot\boldsymbol{J}^2\cdot\mathscr{A}_0)\frac{\boldsymbol{k}_0\cdot\mathscr{S}\cdot\boldsymbol{k}_0}{|\boldsymbol{k}|^4}\right]$$

$$= -2\mathrm{i}\rho\frac{|\boldsymbol{k}_0|}{|\boldsymbol{k}|^2}\left[\boldsymbol{e}\cdot\mathscr{S} - \frac{(\boldsymbol{e}\cdot\mathscr{S}\cdot\boldsymbol{e})|\boldsymbol{k}_0|^2}{|\boldsymbol{k}|^2}\boldsymbol{e}\cdot\boldsymbol{J}^2\right]\cdot\mathscr{A}_0, \tag{17}$$

where $\mathscr{S} \equiv \boldsymbol{J}\cdot\boldsymbol{S}\cdot\boldsymbol{J}$, $\boldsymbol{e} \equiv \boldsymbol{k}_0/|\boldsymbol{k}_0|$ and (4) was used. $\mathscr{A}_0$ is simply the initial solenoidal velocity vector in Fourier space.

The wavenumber spectrum of the initial velocity is defined as

$$S_{0ij}(\boldsymbol{k}_0) = \overline{\mathscr{A}_{0i}\mathscr{A}_{0j}}.$$

For initially isotropic turbulence

$$S_{0ij} = \frac{3q_0^2}{8\pi|\boldsymbol{k}_0|^2}E(|\boldsymbol{k}_0|)(\delta_{ij} - e_i e_j), \tag{18}$$

where $\frac{3}{2}q_0^2$ is the initial turbulent kinetic energy. It follows from this, (9) and (17) that the instantaneous pressure spectrum is

$$\overline{|\hat{p}|^2} = \frac{3q_0^2E(|\boldsymbol{k}_0|)\rho^2}{2\pi|\boldsymbol{k}_0|^4(\boldsymbol{e}\cdot\boldsymbol{J}^2\cdot\boldsymbol{e})^2}\left[\boldsymbol{e}\cdot\mathscr{S} - \frac{\boldsymbol{e}\cdot\mathscr{S}\cdot\boldsymbol{e}}{\boldsymbol{e}\cdot\boldsymbol{J}^2\cdot\boldsymbol{e}}\boldsymbol{e}\cdot\boldsymbol{J}^2\right]\cdot(\boldsymbol{I}-\boldsymbol{e}\boldsymbol{e})\cdot\left[\boldsymbol{e}\cdot\mathscr{S} - \frac{\boldsymbol{e}\cdot\mathscr{S}\cdot\boldsymbol{e}}{\boldsymbol{e}\cdot\boldsymbol{J}^2\cdot\boldsymbol{e}}\boldsymbol{e}\cdot\boldsymbol{J}^2\right]. \tag{19}$$

The bracketed term in (19) is orthogonal to $\boldsymbol{e}$, so the three-term product is equal to the product of the bracketed term with itself.

The pressure variance is the integral over wavenumber of its spectrum:

$$\overline{p'^2} = \int_{-\infty}^{\infty}\overline{|\hat{p}|^2}\,\mathrm{d}^3\boldsymbol{k}_0.$$

Defining

$$L_0^2 = \int_0^{\infty} E(k_0)/k_0^2\,\mathrm{d}k_0 \tag{20}$$

and evaluating the integral in spherical coordinates give

$$\overline{p'^2} = \frac{3q_0^2L_0^2\rho^2}{2\pi}\int_{\Omega}\frac{1}{(\boldsymbol{e}\cdot\boldsymbol{J}^2\cdot\boldsymbol{e})}\times\left[(\boldsymbol{e}\cdot\mathscr{S}^2\cdot\boldsymbol{e}) - 2\frac{(\boldsymbol{e}\cdot\mathscr{S}\cdot\boldsymbol{e})(\boldsymbol{e}\cdot\mathscr{S}\cdot\boldsymbol{J}^2\cdot\boldsymbol{e})}{\boldsymbol{e}\cdot\boldsymbol{J}^2\cdot\boldsymbol{e}} + \frac{(\boldsymbol{e}\cdot\mathscr{S}\cdot\boldsymbol{e})^2(\boldsymbol{e}\cdot\boldsymbol{J}^4\cdot\boldsymbol{e})}{(\boldsymbol{e}\cdot\boldsymbol{J}^2\cdot\boldsymbol{e})^2}\right]\mathrm{d}\Sigma, \tag{21}$$

where the range of integration is the unit sphere: that is, $\boldsymbol{e} = (\cos\theta, \sin\theta\sin\phi, \sin\theta\cos\phi)$ and $\mathrm{d}\Sigma = \sin\theta\,\mathrm{d}\theta\,\mathrm{d}\phi$ with $0 < \theta < \pi$ and $0 < \phi < 2\pi$.

In general this integral must be evaluated numerically. Its behaviour as $t \to 0$ is determined by substituting $\boldsymbol{J} \to \boldsymbol{I}$ to find

$$\overline{p'^2} \to \tfrac{2}{5}(q_0L_0\rho)^2[3\,\mathrm{Tr}(\boldsymbol{S}^2) - (\mathrm{Tr}(\boldsymbol{S}))^2], \tag{22}$$

where Tr(·) means the trace of the matrix argument. Similarly, the limiting behaviour of $\overline{p'^2}$ can be found by differentiating (21) and using $\dot{\boldsymbol{J}} \rightarrow -\boldsymbol{S}$ and $\mathscr{S} \rightarrow -3\boldsymbol{S}^2$:

$$\dot{\overline{p'^2}} \rightarrow -2\mathrm{Tr}(\boldsymbol{S})\overline{p'^2} + \frac{2(q_0 L_0 \rho)^2}{35}[50\,\mathrm{Tr}(\boldsymbol{S})\,\mathrm{Tr}(\boldsymbol{S}^2) - 8(\mathrm{Tr}(\boldsymbol{S}))^3 - 78\,\mathrm{Tr}(\boldsymbol{S}^3)]. \quad (23)$$

Equation (7) can be rewritten

$$\overline{p'\nabla\cdot\boldsymbol{u}'} = -\frac{1}{\rho c^2}(\tfrac{1}{2}\dot{\overline{p'^2}} + \gamma\,\mathrm{Tr}(\boldsymbol{S})\,\overline{p'^2}) \quad (24)$$

because $\dot{P}/P = \gamma\dot{\rho}/\rho = -\gamma\nabla\cdot\boldsymbol{U}$. Substituting (22) and (23) into (24) gives

$$\overline{p'\nabla\cdot\boldsymbol{u}'} \rightarrow \frac{2q_0^2 L_0^2 \rho}{35c^2}[(7\gamma-3)(\mathrm{Tr}(\boldsymbol{S}))^3 - (4+21\gamma)\,\mathrm{Tr}(\boldsymbol{S})\,\mathrm{Tr}(\boldsymbol{S}^2) + 39\,\mathrm{Tr}(\boldsymbol{S}^3)] \quad (25)$$

as $t \rightarrow 0$. This is only the short-time behaviour of the pressure–dilatation correlation; at later times, a general evaluation of the integral (21) is not so easily obtained.

However, it can be evaluated in a simple closed form for the case of one- or two-dimensional axisymmetric compressions. For the one-dimensional compression $J_2 = J_3 = 1$ and $S_2 = S_3 = 0$. Then

$$\overline{p'^2} = 6(q_0 L_0 \rho)^2 \mathscr{S}_1^2 F(\alpha), \quad (26)$$

where $\alpha = J_1^2 - 1$ and

$$F(x) = \frac{(x-1)\tan^{-1}x^{\frac{1}{2}}}{16x^{\frac{5}{2}}} + \frac{3x^2+2x+3}{48x^2(1+x)^2}. \quad (27)$$

In this case $\rho = J_1\rho_0$ and $\mathscr{S}_1 = a_1 J_1^3$ (see the equations following (4) and (17)) so

$$\overline{p'^2} = 6(q_0 L_0 \rho_0 a_1)^2 J_1^8 F(\alpha).$$

The term in parentheses is a dimensional constant; the other terms determine the dependence of $\overline{p'^2}$ on compression ratio, J_1. For a two-dimensional axisymmetric compression $J_1 = 1$, $J_3 = J_2$ and $S_1 = 0$. In this case

$$\overline{p'^2} = 6(q_0 L_0 \rho_0 a_2)^2 J_2^2 F(\beta), \quad (28)$$

where $\beta = J_2^{-2} - 1$. Note that the vortical pressure fluctuation is produced by straining, and vanishes when $a_2 = 0$. The corresponding pressure dilatation can be evaluated by substituting (28) into (7); it is easier to do this by numerical evaluation of the derivative with respect to time than to differentiate (26) and (28) analytically.

Figure 1 shows the turbulent intensities, normalized by their initial value, for one- and two-dimensional compression. They were evaluated from the formulae

$$\left.\begin{aligned} \frac{\overline{u_1'^2}}{q_0^2} &= \tfrac{3}{4}J_1^2 G(\alpha) \\ \frac{\overline{u_2'^2}}{q_0^2} &= \tfrac{3}{8}\left(1 - \frac{1}{\alpha} + \frac{J_1^4}{\alpha^{\frac{3}{2}}}\tan^{-1}\alpha^{\frac{1}{2}}\right) \end{aligned}\right\} \text{one-dimensional}, \quad (29a)$$

$$\left.\begin{aligned} \frac{\overline{u_1'^2}}{q_0^2} &= \tfrac{3}{4}G(\beta) \\ \frac{\overline{u_2'^2}}{q_0^2} &= \tfrac{3}{8}J_2^2\left(1 - \frac{1}{\beta} + \frac{\tan^{-1}\beta^{\frac{1}{2}}}{J_2^4\beta^{\frac{3}{2}}}\right) \end{aligned}\right\} \text{two-dimensional}, \quad (29b)$$

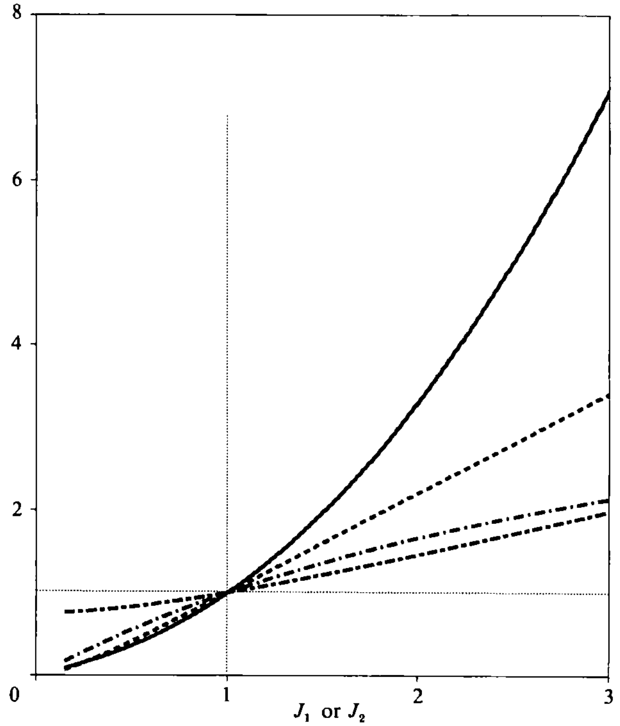

FIGURE 1. Turbulent intensities versus linear compression ratio: one- and two-dimensional axisymmetric compressions. ---, $\overline{u_1^2}$ (1-D); —-—, $\overline{u_2^2}$ (1-D); —·—·, $\overline{u_1^2}$ (2-D); ——, $\overline{u_2^2}$ (2-D).

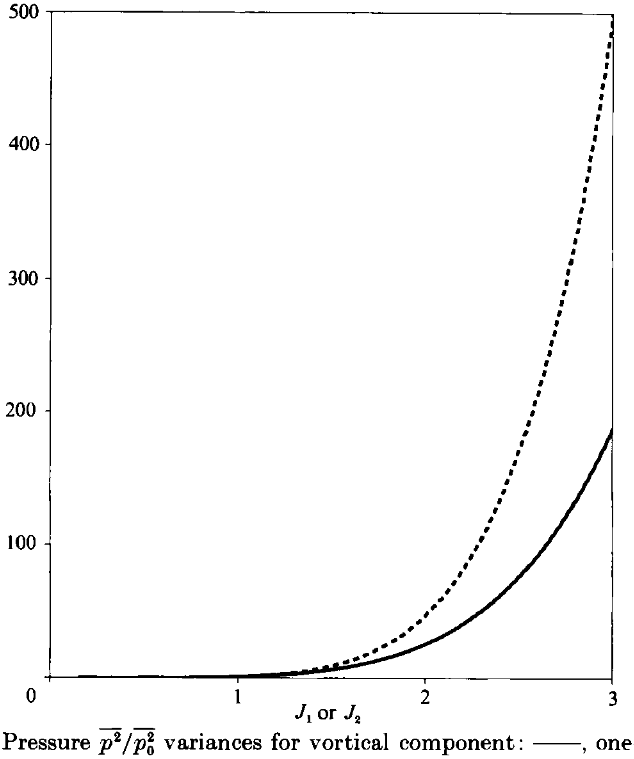

FIGURE 2. Pressure $\overline{p^2}/\overline{p_0^2}$ variances for vortical component: ——, one-dimensional; ---, two-dimensional.

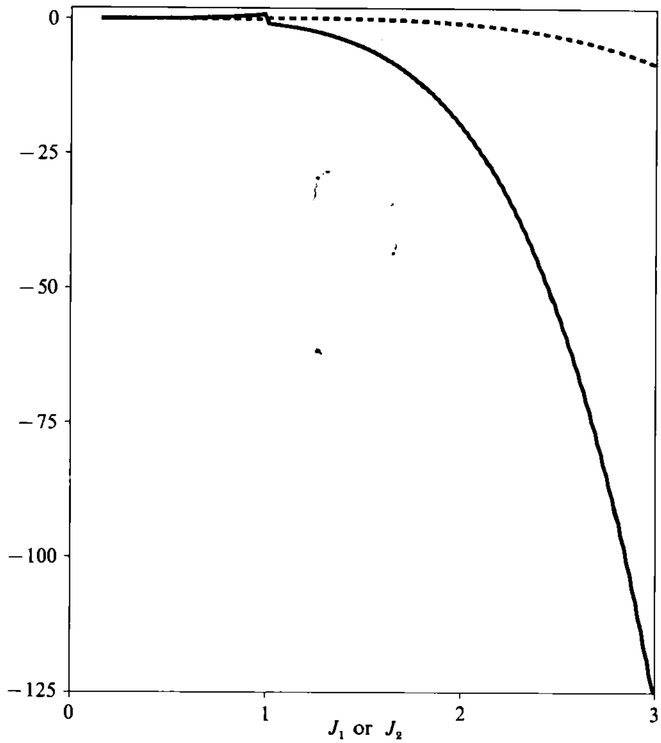

FIGURE 3. Pressure–dilatation correlation for $\overline{p\theta}$ vertical component: ——, one-dimensional; – – –, two-dimensional.

where
$$G(x) = \frac{1}{x} + \frac{x-1}{x^{\frac{3}{2}}} \tan^{-1} x^{\frac{1}{2}},$$

taken from Ribner & Tucker (1953). Because the turbulence is axisymmetric, $\overline{u_3'^2} = \overline{u_2'^2}$. The abscissa of figure 1 is J_1 or J_2; hence, this axis is the volumetric compression ratio in one dimension and the square root of the compression ratio in two dimensions. Values of the abscissa of less than unity correspond to volumetric expansion, and values greater than unity to compression.

Figures 2 and 3 show the present results for $\overline{p'^2}$ and $\overline{p'\nabla \cdot u'}$; for the latter $\gamma = 1.4$ was used. The former is normalized by its initial value, $\overline{p_0'^2} = \frac{4}{5} q_0^2 L_0^2 \rho_0^2 a^2$; the latter is normalized by $-\overline{p_0'^2}\, a/\rho_0 c_0^2$. a represents either a_1 or a_2, as defined by (2). Note that $a < 0$ for a compression, so the constant by which $\overline{p'\nabla \cdot u'}$ is normalized is positive in this case. The apparent discontinuity at $J = 1$ in figure 3 simply is a consequence of the normalization constant varying as a^3 as $a \rightarrow 0$.

Comparing figures 1 and 2, one sees that compression has a rather greater effect on pressure fluctuations than on velocity fluctuations; indeed, the magnitude of the effect of compression on pressure fluctuations is disconcertingly large. Numerical simulations of compressed turbulence (Coleman & Mansour 1991) show a similarly large effect. This disproportionate effect on pressure fluctuations explains the importance of pressure fluctuations and pressure–dilatation correlations in turbulent flow through shock waves and in other flows with rapid compression. Although the effect of compression seems greater in two dimensions, it should be appreciated that when $J = 3$ the volumetric compression is 9-fold in two dimensions, but only 3-fold

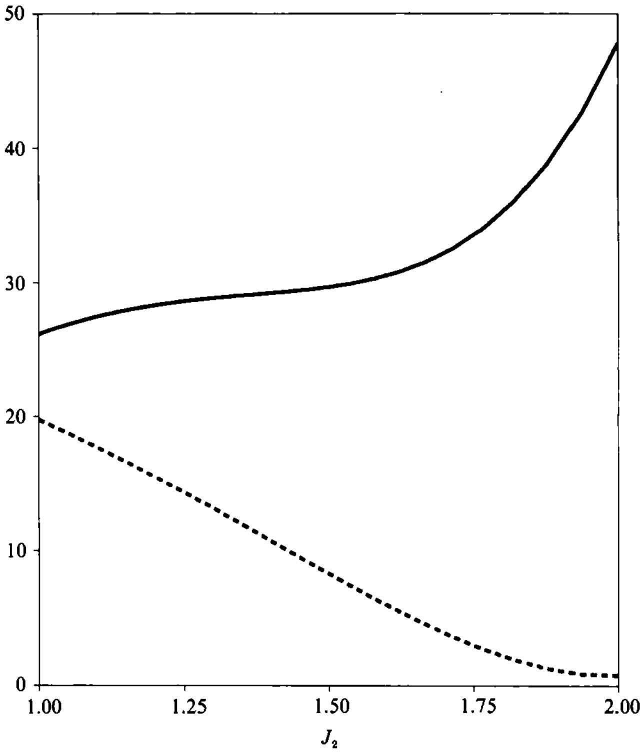

FIGURE 4. Pressure variance $\overline{p^2}$ (——) and pressure dilatation $\overline{p\theta}$ (---) associated with the vortical mode for compression with $J_1 = 2$, $J_3 = 1$ as a function of J_2.

in one dimension; for a given volumetric compression ratio the one-dimensional compression gives rise to a greater pressure fluctuation. Figure 3 shows that the pressure–dilatation correlation is significantly larger for the one-dimensional compression. Recall that for a three-dimensional, spherically symmetric compression the vortical contribution to $\overline{p'^2}$ and $\overline{p'\nabla\cdot\boldsymbol{u}'}$ is identically zero. Hence, the pressure dilatation decreases with increasing dimensionality of the compression.

For asymmetric compressions (21) can be evaluated numerically. Figure 4 shows such an evaluation for a compression with $J_1 = 2$, $J_3 = 1$ and J_2 varying along the abscissa. When $J_2 = 1$ the one-dimensional axisymmetric result is recovered, and when $J_2 = 2$ the two-dimensional cylindrically symmetric result is obtained. In figure 5 the compression is axisymmetric, with $J_1 = 2$ and $J_3 = J_2$ varying along the abscissa. This curve interpolates between a one-dimensional compression and a spherically symmetric compression. Recall that the latter has $\overline{p'^2} \equiv 0$. In broad terms, increasing the symmetry of the distortion decreases the pressure–dilatation correlation. The pressure variance does not show a correspondingly simple, monotonic variation: in figure 4 is increases with increasing symmetry, while in figure 5 it first increases, then decreases to its value of zero for spherical compression.

A quasi-homogeneous calculation, making use of the above strictly homogeneous analysis is presented in Appendix A. That Appendix describes distortion of turbulence by flow through a nozzle. The strain and compression are more complex than for homogeneous compressions: the turbulence is expanded along the axis of the nozzle and compressed in the perpendicular direction. The mean rate of strain increases from zero as the contracting section is entered, then decreases to zero as it

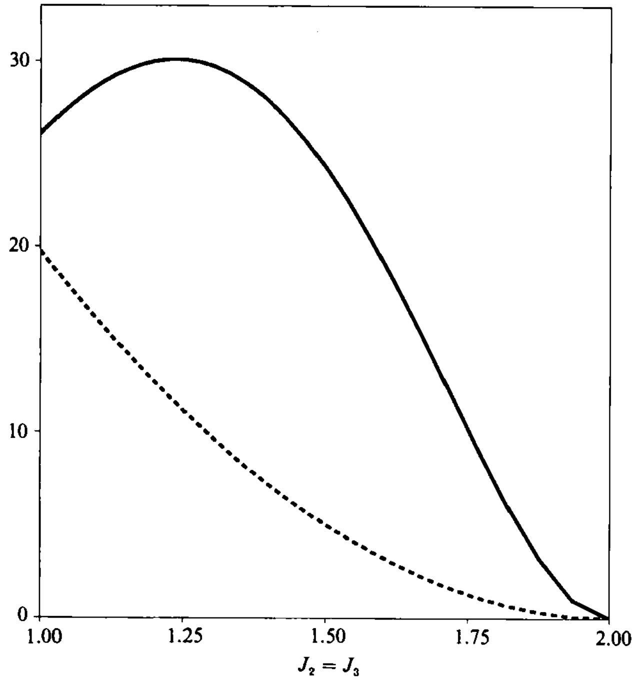

FIGURE 5. Pressure variance $\overline{p^2}$ (——) and pressure dilatation $\overline{p\theta}$ (----) of vortical mode for axisymmetric compression with $J_1 = 2$ versus J_2.

is exited. Figure 12 shows how the pressure variance rises and falls through the nozzle, along with the corresponding behaviour of pressure dilatation. This is analogous to what Lee *et al.* (1991) observed in flow through a shock wave, although the nozzle presents a rather milder version.

5. Acoustic mode

The results presented so far are for the vortical component of the random velocity field. In general, compressed acoustic waves will also be present. In the current limit of small Δm the acoustic frequency is high – of $O(1/\Delta m)$ on the timescale of the compression. To lowest order of approximation ϕ_1 is given by the solution to

$$\frac{\mathrm{d}}{\mathrm{d}t}(c^{-2}\dot{\phi}_1) + |\boldsymbol{k}|^2\phi_1 = 0 \tag{30}$$

(see the discussion below (15)). The acoustic field is generated entirely by its initial condition because (30) is a homogeneous equation. Also, it is consistent with the high-frequency limit to solve (30) by a WKB approximation (Bender & Orszag 1978). Compression will increase c^2 and decrease the wavelength of the acoustic disturbance; we wish to determine how these affect the statistics of a field of random waves.

The WKB solution to (30) is

$$\phi_1 = \left(\frac{c}{|\boldsymbol{k}|}\right)^{\frac{1}{2}} (a \sin \Theta + b \cos \Theta), \tag{31}$$

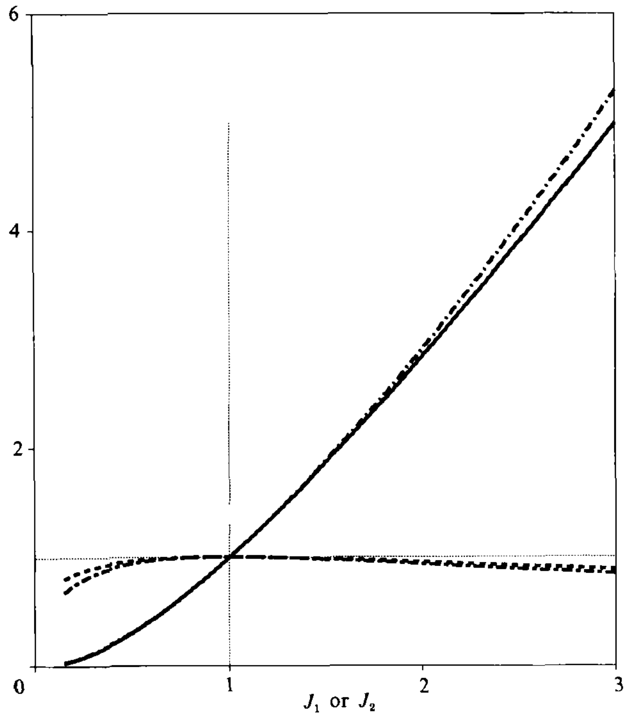

FIGURE 6. Turbulent intensities of acoustic mode: ——, $\overline{u_1^2}$ (1-D); ---, $\overline{u_1^2}$ (2-D); —·—, $\overline{u_2^2}$ (1-D); —·—·, $\overline{u_2^2}$ (2-D).

where $$\Theta = \int_0^t |\boldsymbol{k}|\, c\, \mathrm{d}t, \quad a = \dot{\phi}_1(0)/(|\boldsymbol{k}|\, c_0^3)^{\frac{1}{2}}; \quad b = \phi_1(0)/(|\boldsymbol{k}|/c_0)^{\frac{1}{2}}.$$

It is assumed that the initial conditions of the acoustic field are uncorrelated with those of the solenoidal, vortical field. Then the acoustic components of the velocity correlation tensor are

$$(\overline{u_i u_j})_{\mathrm{a}} = \int \frac{k_i k_j c}{2|\boldsymbol{k}|}[\overline{a^2}+\overline{b^2}+(\overline{b^2}-\overline{a^2})\cos 2\Theta + 2\overline{ab}\sin 2\Theta]\, \mathrm{d}^3\boldsymbol{k}_0.$$

By the reasoning given previously, the frequency of the oscillatory terms is high when $t > 0$ (i.e. $\Theta = \int \omega\, \mathrm{d}t \sim O(1/\Delta m)$ when t is of order the distortion timescale). It follows that their contribution to the integral is $O(\Delta m^4)$ smaller than the non-oscillatory terms. Hence, to leading order,

$$(\overline{u_i u_j})_{\mathrm{a}} = c \int (\overline{a^2}+\overline{b^2}) \frac{k_i k_j}{2|\boldsymbol{k}|}\, \mathrm{d}^3\boldsymbol{k}_0. \tag{32}$$

If we define $$3q_{\mathrm{a}}^2 = 2\pi c_0 \int_0^\infty (\overline{a^2}+\overline{b^2})\, k_0^3\, \mathrm{d}k_0 \tag{33}$$

then $$(\overline{\boldsymbol{uu}})_{\mathrm{a}} = \frac{3q_{\mathrm{a}}^2 c}{4\pi c_0} \int_\Omega \frac{(\boldsymbol{e}\cdot\boldsymbol{J})(\boldsymbol{e}\cdot\boldsymbol{J})}{(\boldsymbol{e}\cdot\boldsymbol{J}^2\cdot\boldsymbol{e})^{\frac{1}{2}}}\, \mathrm{d}\Sigma; \tag{34}$$

$\frac{3}{2}q_{\mathrm{a}}^2$ is the initial kinetic energy of the acoustic field. The integrals over the unit sphere can again be evaluated for one- and two-dimensional axisymmetric compressions. After substituting either $c = J_1^{(\gamma-1)/2}$ or $c = J_2^{\gamma-1}$ for one- or two-dimensional compressions, the results

$$\left.\begin{aligned} \frac{(\overline{u_1'^2})_a}{q_a^2} &= \tfrac{3}{2} J_1^{(\gamma+3)/2} H(\alpha) \\ \frac{(\overline{u_2'^2})_a}{q_a^2} &= \tfrac{3}{4} J_1^{(\gamma-1)/2}\left(\frac{2\sinh^{-1}\alpha^{\frac{1}{2}}}{\alpha^{\frac{1}{2}}} - H(\alpha)\right) \end{aligned}\right\} \text{ one-dimensional,} \tag{35a}$$

$$\left.\begin{aligned} \frac{(\overline{u_1'^2})_a}{q_a^2} &= \tfrac{3}{2} J_2^{\gamma-2} H(\beta) \\ \frac{(\overline{u_2'^2})_a}{q_a^2} &= \tfrac{3}{4} J_2^{\gamma}\left(\frac{2\sinh^{-1}\beta^{\frac{1}{2}}}{\beta^{\frac{1}{2}}} - H(\beta)\right) \end{aligned}\right\} \text{ two-dimensional,} \tag{35b}$$

where $$H(x) = [(x+x^2)^{\frac{1}{2}} - \sinh^{-1} x^{\frac{1}{2}}]/x^{\frac{3}{2}}$$

are obtained. These are the intensities of compressed acoustic waves. The corresponding pressure variance is obtained from (31) and $\overline{p'^2} = \rho^2 \overline{\dot{\phi}^2}$. Again, we invoke the present high-frequency limit and drop the higher-order contribution from oscillatory components of the integrand:

$$\overline{p_a'^2} = \tfrac{1}{2}\rho^2 c^3 \int (\overline{a^2} + \overline{b^2})|\boldsymbol{k}|\, \mathrm{d}^3|\boldsymbol{k}_0| = \frac{3\rho^2 q_a^2 c^3}{4\pi c_0} \int_\Omega (\boldsymbol{e}\cdot\boldsymbol{J}^2\cdot\boldsymbol{e})^{\frac{1}{2}} \mathrm{d}\Sigma. \tag{36}$$

As $t \to 0$, $$\overline{p_a'^2} \to 3\rho^2 q_a^2 c^3/c_0$$

and $$\overline{\dot{p}_a'^2} \to -\tfrac{1}{6}(9\gamma+5)\,\overline{p_a'^2}\,\mathrm{Tr}(\boldsymbol{S}). \tag{37}$$

The relation (37), between $\overline{\dot{p}_a'^2}$ and $\overline{p_a'^2}$, is valid for all t for a spherically symmetric compression (Sabelnikov 1975; Zeman 1991). Note, in particular, that the acoustic pressure variance is not zero for spherical compression. Indeed, because $\mathrm{Tr}(\boldsymbol{S}) = \boldsymbol{\nabla}\cdot\boldsymbol{U}$, (37) is the same as $\overline{p_a'^2}/\overline{p_{a_0}'^2} \to (\rho/\rho_0)^{(9\gamma+5)/6}$ as $t \to 0$.

Again, (36) can be evaluated in closed form for one- and two-dimensional compressions:

$$\overline{p_a'^2} = 3(\rho_0 c_0 q_a)^2 \frac{J_1^{(3\gamma+1)/2}}{2\alpha^{\frac{1}{2}}}[\sinh^{-1}\alpha^{\frac{1}{2}} + (\alpha^2+\alpha)^{\frac{1}{2}}] \quad \text{one-dimensional,} \tag{38a}$$

$$\overline{p_a'^2} = 3(\rho_0 c_0 q_a)^2 \frac{J_2^{3\gamma+2}}{2\beta^{\frac{1}{2}}}[\sinh^{-1}\beta^{\frac{1}{2}} + (\beta^2+\beta)^{\frac{1}{2}}] \quad \text{two-dimensional.} \tag{38b}$$

Note that when the strain vanishes ($\alpha = \beta = 0$) (38) reduces to the equipartition value $\overline{p_a'^2} = 3\rho_0^2 c_0^2 q_a^2$.

Figures 6, 7 and 8 are plots of the acoustic solution. Figure 6 shows that the variance of the velocity component in the direction of compression is increased by compression. Figures 7 and 8 show how the two-dimensional compression causes rather large increases in pressure variance and in pressure–dilatation correlation. Recall that J_1 and J_2^2 are the volumetric compression ratios. Hence, the levels of pressure variance and pressure dilatation in the two cases shown are similar for a given *volumetric* compression. By contrast, the vortical contribution to pressure–

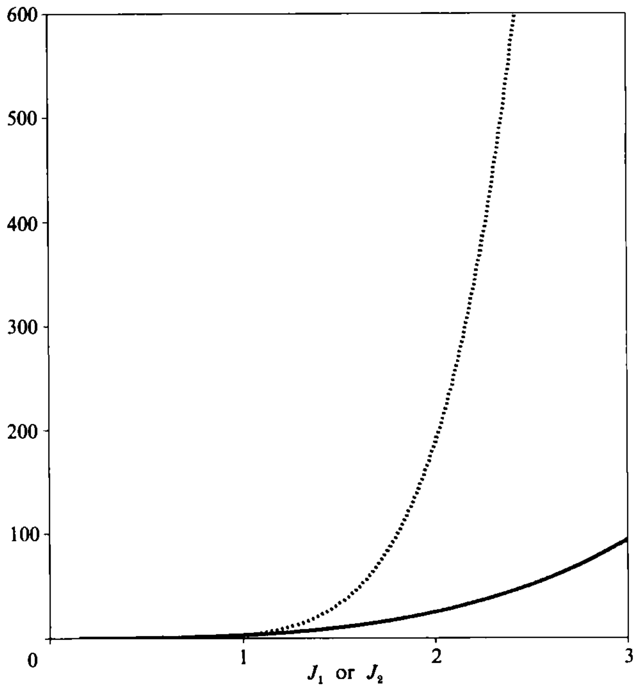

FIGURE 7. Pressure variance of acoustic mode $\overline{p^2}/\overline{p_0^2}$: ——, one-dimensional; ....., two-dimensional.

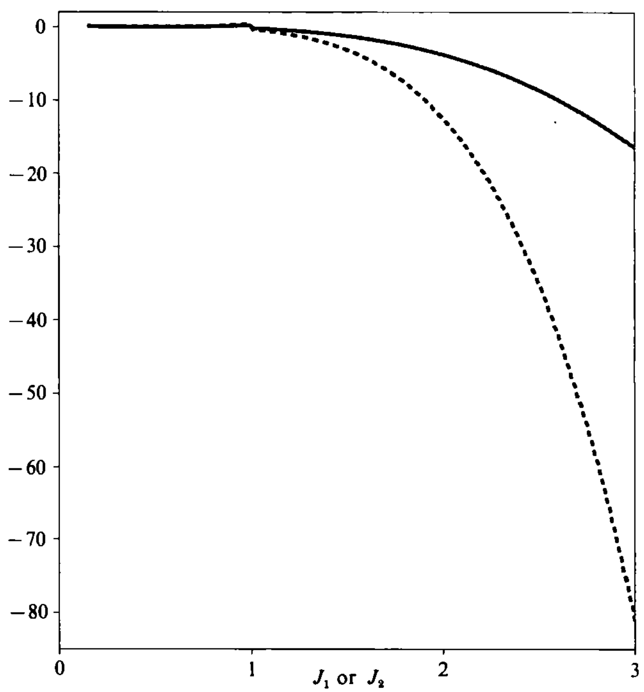

FIGURE 8. Pressure–dilatation of the acoustic mode. $\overline{p\theta}$: ——, one-dimensional; ----, two-dimensional.

dilatation (figure 3) was far greater for the one-dimensional case. The short-time relation (37) suggests that the acoustic pressure variance should depend primarily on the mean density, and hence on the net volumetric compression.

6. Turbulence modelling

The short-time behaviour of rapid distortion solutions is sometimes used as guidance to turbulence closure modelling. It will be used here to model the pressure–dilatation correlation. As noted in the introduction, this correlation can be a significant drain of turbulent kinetic energy in high-speed, non-equilibrium flows.

When the initial condition is of isotropy, then RDT provides a means of perturbing the isotropic symmetry. A general approach to model formulation consists of expanding in powers of anisotropy (Launder, Reece & Rodi 1975). Thus, RDT provides concrete results which are consistent with a more abstract formalism. We will formulate our model by applying both the general formalism, and the concrete RDT analysis.

The Favré-averaged kinetic energy equation contains the term (Zeman 1991) $\Pi_{\mathrm{d}} \equiv \overline{p\boldsymbol{\nabla}\cdot\boldsymbol{u}'}/\bar{\rho}$, which requires modelling. The present analysis suggests that a model might make use of (7). In general, nonlinear terms in the fluctuating continuity equation must be added; however, (7) is remarkably well satisfied in numerical simulations (Blaisdell, Mansour & Reynolds 1991), and Π_{d} is important primarily when the turbulence evolves in consequence of rapid distortion by the mean flow, so such terms will be omitted here. To use (7) for Π_{d}, formulae for the pressure variance are required. It will be assumed that acoustic and solenoidal contributions to $\overline{p'^2}$ are statistically independent: $\overline{p'^2} = \overline{p_{\mathrm{a}}'^2} + \overline{p_{\mathrm{s}}'^2}$. In numerical cimulations, these contributions are coupled by initial conditions, so the independence assumption can only be true after a transient. Also, when Δm^2 is not small the acoustic mode will be coupled to the vorticity through the forcing term on the right-hand side of (15): in this case there can be no separation into uncorrelated acoustic and solenoidal components. If L is estimated by the usual formula $L \sim k^{\frac{3}{2}}/\epsilon$ then $\Delta m = (|a|k/\epsilon)(k^{\frac{1}{2}}/c)$. The first factor is the ratio of turbulence to distortion timescales and must be large in the rapid distortion approximation. The second factor is the fluctuation Mach number and must be small if the present independence assumption is to have validity. When the fluctuation Mach number is not sufficiently small the RDT analysis requires solution of (15), or (13), without dropping the vortical forcing of acoustic disturbances. That presents a formidable problem, with which we have so far made no progress.

The relation (37) was used by Zeman (1990) to model the evolution of acoustic pressure fluctuations. Although he gave the justification that the expression followed from Sabelnikov's (1975) rapid distortion analysis of spherical compression, we now see that this equation applies (as $t \rightarrow 0$) to more general compressions. Zeman also allowed for relaxation to a non-zero equilibrium level of pressure fluctuations, so his model is

$$\dot{\overline{p_{\mathrm{a}}'^2}} = -\frac{(9\gamma+5)}{6}\overline{p_{\mathrm{a}}'^2}\,\mathrm{Tr}\,(\boldsymbol{S}) + \frac{p_{\mathrm{e}}^2 - \overline{p_{\mathrm{a}}'^2}}{\tau_{\mathrm{a}}}, \tag{39}$$

where τ_{a} is an acoustic relaxation timescale and p_{e}^2 is the equilibrium pressure variance.

The rapid contribution to the solenoidal pressure variance will be modelled by making use of (22) and (23). Because (23) is not the time derivative of (22), it is necessary to include the next term in the short-time expansion of (21). This can be done by the previously cited method of expanding about isotropy (Launder *et al.* 1975). That method yields the general result

$$\overline{p_s'^2} = (\rho q L)^2 [C_1 \operatorname{Tr}(\boldsymbol{S}_*^2) + C_2 b_{ij} S^2_{*_{ij}}] + O(\|\boldsymbol{b}\|^2), \tag{40}$$

in which b_{ij} is the anisotropy tensor $\overline{u_i u_j}/q^2 - \delta_{ij}$; $S_{*ij} \equiv S_{ij} - \frac{1}{3}\delta_{ij}\operatorname{Tr}(\boldsymbol{S})$; and C_1 and C_2 are constants (strictly, C_1 can depend linearly on $\boldsymbol{b}$, through its invariants, and one might propose that C_1 and C_2 be made functions of Δm). When equation (40) is regarded as a turbulence model, q and L represent instantaneous values, rather than the initial values appearing in (22). The RDT values for the constants are found by comparing (40) to (23), after substituting the short-time behaviour $\boldsymbol{b} \rightarrow -4/5\boldsymbol{S}_* t$ and $\mathrm{d}(qL)/\mathrm{d}t \rightarrow O(t)$. This yields $C_1 = \frac{6}{5}$ and $C_2 = \frac{18}{7}$. These are the constants which reproduce the short-time RDT solution; but this solution is not necessarily representative of the later evolution of the pressure–dilatation correlation. It might be expected that somewhat different values would result from fitting the model (7), (39) and (40) to numerical or experimental data. Also, there is some uncertainty in how to determine a model value of L: turbulence models are usually based on the dissipation length q^3/ϵ; however in (40) L is a scale associated with pressure fluctuations (see (20)). Despite these caveats, in the calculation described below, the RDT values of C_1 and C_2 were found to give a very reasonable prediction of Π_d.

For completeness it will be noted that when the mean rotation, $\Omega_{ij} = \frac{1}{2}(\partial_i U_j - \partial_j U_i)$, is not zero, the procedure used to obtain (40) yields

$$\overline{p_s'^2} = (\rho q L)^2 [C_1(\operatorname{Tr}(\boldsymbol{S}_*^2) + \tfrac{5}{3}\operatorname{Tr}(\boldsymbol{\Omega}^2)) + b_{ij}\{C_2(S^2_{*_{ij}} + \Omega^2_{ij}) + C_3(S_{*ik}\Omega_{kj} + S_{*jk}\Omega_{ki})\}].$$

This contains a third constant.

The present rapid pressure–dilatation formulation, (7), (39) and (40), was incorporated into the second-order closure model of Zeman (1990, 1991). The model equations are contained in Appendix B. They have been simplified to the case of one-dimensional homogeneous compression. For the most part the model is of the type used for incompressible flow, with two notable exceptions. Firstly, (B 4) was used to rewrite the kinetic energy equation as a 'total fluctuation energy' equation: the notation Y is used for this total energy. Secondly, a lengthscale equation is included; this equation was formulated by Zeman (1991) to account for the lengthscale reduction which occurs in a rapid compression. By design, in decaying turbulence L reduces to the dissipative scale $(2k)^{\frac{3}{2}}/\epsilon$.

Figure 9 shows a computation with the present model, along with numerical simulation data provided by Dr G. N. Coleman. The simulation is of initially isotropic turbulence subjected to homogeneous, one-dimensional compression. At the initial time in this simulation $|a|k/\epsilon = 23.5$ and $k/c = 0.017$, so $\Delta m \approx 0.4$; thus, the requirement that $\Delta m^2 \ll 1$ is met. Further information on the simulation can be found in Coleman & Mansour (1991), where it is listed as case c1db. The agreement between the present model and the data is quite satisfactory, although the steep rises of production, Π_d and kinetic energy, k, occur somewhat later in the model than in the data. Both the model and data show that after a non-dimensional time of 0.3, the pressure–dilatation term is consistently about 15% as large as the production term. Thus the pressure dilatation causes a significant drain of kinetic energy into pressure variance.

As noted in the Appendix B, the constants of the rapid pressure–strain model are slightly smaller here than in Zeman (1990). These lower values were required to achieve a satisfactory level of anisotropy $(\overline{u_1^2}/2k)$ and, consequently, to give a

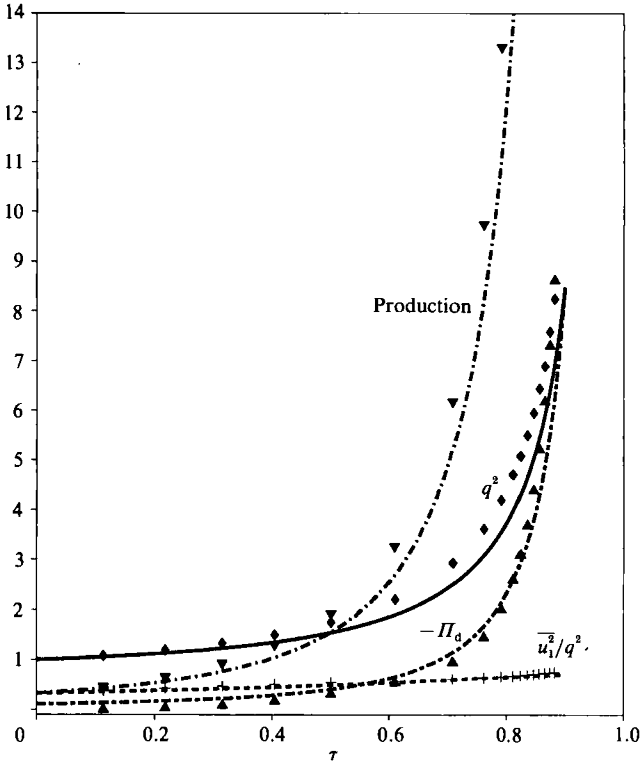

FIGURE 9. Comparison of model (lines) to DNS data (symbols).

satisfactory level of energy production $(-\overline{u_1^2}\partial_1 U_1)$. Even lower values of these constants would improve the agreement in figure 9. However, the purpose of this figure is simply to show that the present model for Π_d gives reasonable results. In the model, Π_d is not zero initially, while the initial conditions of the simulation make it zero. As we have noted, this would imply that the solenoidal and acoustic pressures cancel at the outset, so the assumption that they are uncorrelated is not valid $(\overline{p_a p_s} \neq 0)$ during a brief initial period.

The model and data for dissipation rate, ϵ, are not shown in figure 9 because they are very small in comparison to the other terms in the kinetic energy equation. This is so because the compression is rapid: initially $\nabla \cdot Uk/\epsilon$ is equal to 23.5, so the production is an order of magnitude larger than dissipation. As the compression proceeds, the ratio of production to dissipation increases considerably: at $\tau = 0.8$, $-\overline{u_1^2}\partial_1 U_1/\epsilon = 123.1$ and $-\Pi_d/\epsilon = 18.5$.

Finally, we remark that in a previous effort to account for the effect of non-spherical compression, Zeman (1991) suggested a rapid contribution to Π_d of the form

$$\Pi_d \propto -\frac{(\overline{p'^2})^{\frac{1}{2}}}{PM_T^2}\frac{k^2}{\epsilon}\mathrm{Tr}(\boldsymbol{S}_*^2). \tag{41}$$

Since $\overline{p'^2}$ varies as $\boldsymbol{S}_*^2$, (41) varies as $\mathbf{S}_*^3$, which agrees with the short-time RDT result (25). In this respect, the present analysis lends formula (41) some support. An alternative algebraic model might be arrived at by dropping the differentiated term from (B 4); however, that may be an unsatisfactory approximation in rapidly evolving flows.

7. Discussion

Rapid distortion theory was investigated here for the insight that it gives into the behaviour of turbulence subjected to homogeneous compression. The analysis and closure modelling are restricted to low fluctuating Mach numbers because nonlinear compressible phenomena were neglected. More importantly, the linear analysis was done only in the limit $\Delta m^2 \ll 1$. This enables the neglect of coupling between acoustic and vortical components at lowest order of approximation. The only higher-order effect considered here is the generation of a non-zero pressure–dilatation correlation at next order of approximation. When Δm is not small, distortion of vorticity can contribute significantly to the acoustic mode. It should be emphasized that the case of $\Delta m = O(1)$ is still within the purview of RDT, but the analysis would be rather difficult.

Spherically symmetric distortions produce no (rapid) solenoidal pressure because $\boldsymbol{J}$ is then proportional to the identity matrix, so the source term $\boldsymbol{k}\cdot\boldsymbol{\mathscr{A}}$ is proportional to $\boldsymbol{k}_0\cdot\boldsymbol{\mathscr{A}}_0 = 0$ (recall that $\boldsymbol{\mathscr{A}}_0$ is the initial solenoidal velocity); i.e. orthogonality of $\boldsymbol{k}$ and $\boldsymbol{\mathscr{A}}$ is preserved by the spherical symmetry. For asymmetrical compression the distorted wave vector will not remain orthogonal to $\boldsymbol{\mathscr{A}}$: this is how solenoidal pressure fluctuations arise in the present formulation.

These considerations apply quite generally to the source term in (13). Irrespective of the magnitude of Δm, this term vanishes for spherically symmetric distortions and the acoustic component is uncoupled from the vorticity. The term 'acoustic component' refers to the homogeneous solution of (15), or if $\boldsymbol{k}\cdot\boldsymbol{\mathscr{A}} = 0$, to the solution of (13). Such solutions depend on the distortion only through the time-dependence of c and $|\boldsymbol{k}|$; hence they are non-zero for spherical compression and are affected by such compression.

The closure model for pressure dilatation, equations (7) and (40), explicitly invokes the small-Δm lowest-order decoupling of acoustic and solenoidal components. Again, the only higher-order effect considered is the generation of pressure–dilatation correlation by the solenoidal component. The model was formulated by reference to the RDT analysis; essentially the short-time expansion of (21) to $O(t)$ was rescaled to produce a model which was assumed valid for all t. The expansion of $\overline{p_s'^2}$ had to contain $O(t)$ terms to obtain the correct behaviour (25) for $\overline{p'\boldsymbol{\nabla}\cdot\boldsymbol{u}'}$. The rescaling consisted of replacing initial values of q and L by instantaneous values and of eliminating $S_{ij}t$ in favour of b_{ij}. Of course this particular procedure has to result in a formula consistent with the general procedure of expanding about isotropy; but because it is accomplished by expanding a solution to the governing equations, coefficients which are indeterminate in the general procedure are determined. It is remarkable that this approach leads to a model which is able to predict the turbulence statistics at large times, when the short time expansion is invalid.

We are grateful to Dr G. N. Coleman for graciously providing us with his DNS data.

Appendix A. The quasi-homogeneous approximation

It was remarked in the introduction that the present solution is valid as a quasi-homogeneous approximation to non-homogeneously distorted turbulence. All that is required is to relate $\boldsymbol{J}$ and $\boldsymbol{S}$ to suitable distortion and rate-of-strain tensors for the

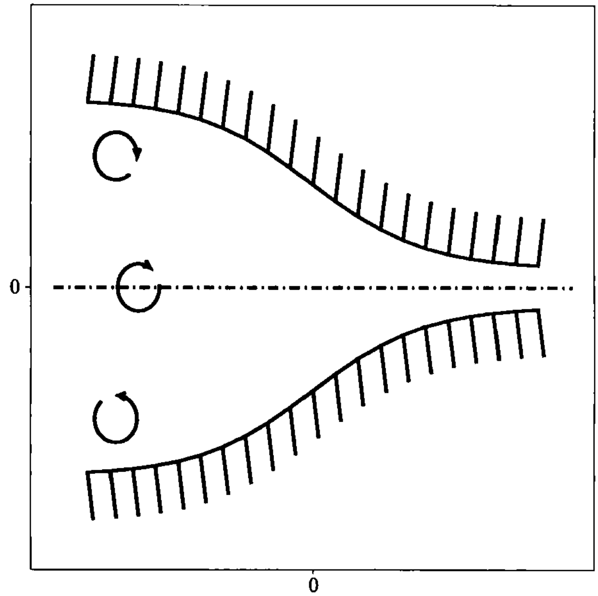

FIGURE 10. Turbulent flow through a nozzle.

mean potential flow. A method for doing so is described in Hunt (1973) for two-dimensional distortions and in Durbin (1981) for axisymmetric distortions. Along a symmetry line, such as the centreline of the nozzle illustrated in figure 10, the following simple forms are obtained:

$$\boldsymbol{J} = \begin{pmatrix} 1/U & 0 & 0 \\ 0 & \rho U & 0 \\ 0 & 0 & 1 \end{pmatrix}, \quad \boldsymbol{S} = \begin{pmatrix} \partial_x U & 0 & 0 \\ 0 & -\partial_x(\rho U)/\rho & 0 \\ 0 & 0 & 0 \end{pmatrix} \tag{A 1}$$

for a two-dimensional nozzle, and

$$\boldsymbol{J} = \begin{pmatrix} 1/U & 0 & 0 \\ 0 & (\rho U)^{\frac{1}{2}} & 0 \\ 0 & 0 & (\rho U)^{\frac{1}{2}} \end{pmatrix}, \quad \boldsymbol{S} = \begin{pmatrix} \partial_x U & 0 & 0 \\ 0 & -\partial_x(\rho U)/2\rho & 0 \\ 0 & 0 & -\partial_x(\rho U)/2\rho \end{pmatrix} \tag{A 2}$$

for an axisymmetric nozzle. One-dimensional isentropic gas dynamics will be used to determine U and ρ for a two-dimensional nozzle with cross-section given by $A(x)/A_\infty = (1+0.3e^x)/(1+e^x)$. The Mach number, m, is determined as a function of x by

$$mA/(1+\tfrac{1}{2}(\gamma-1)\,m^2)^{(\gamma+1)/2(\gamma-1)} = m_\infty A_\infty/(1+\tfrac{1}{2}(\gamma-1)\,m_\infty^2)^{(\gamma+1)/2(\gamma-1)}, \tag{A 3}$$

which is the condition ρUA = constant. Once m is found then

$$c^2/c_\infty^2 = (1+\tfrac{1}{2}(\gamma-1)\,m_\infty^2)/(1+\tfrac{1}{2}(\gamma-1)\,m^2), \quad U = mc, \quad \rho/\rho_\infty = (c^2/c_\infty^2)^{1/(\gamma-1)}$$

can be determined.

In the quasi-homogeneous approximation, the acoustic component is identically zero if it vanishes upstream. In this case only the vortical mode exists within the contraction (assuming no entropy fluctuations), so (21) describes the pressure fluctuation. For the calculations in figures 11 and 12, $\gamma = 1.4$ and $m_\infty = 0.04$ were

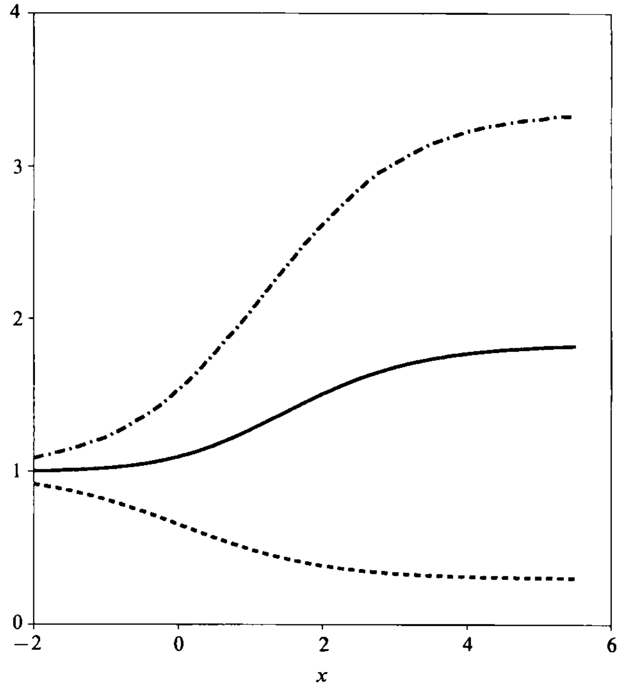

FIGURE 11. Prescribed area ratio A/A_∞ (– – – –) and Mach number distribution m/m_∞ (—·—·), and resulting evolution of turbulent intensity q^2 (——).

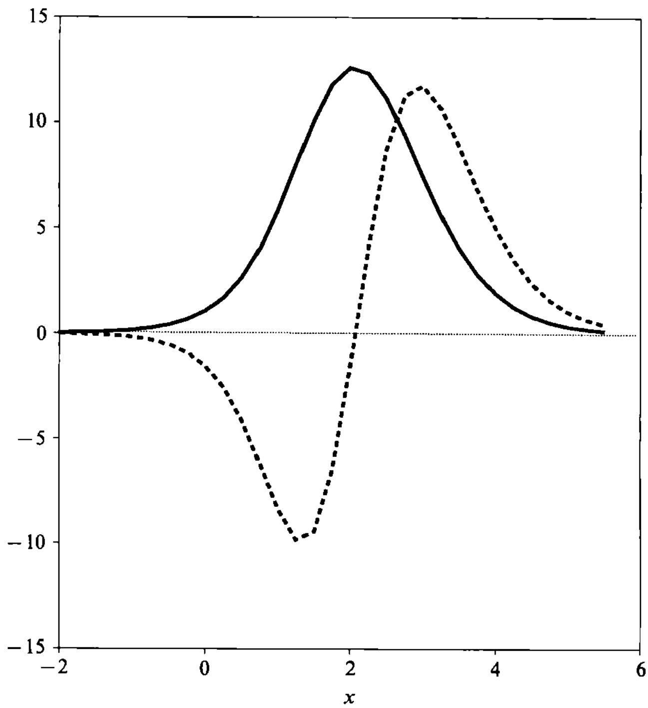

FIGURE 12. Evolution of pressure $\overline{p^2}$ (——) and pressure–dilatation $\overline{p\theta}$ (– – – –) down the nozzle contraction.

used. Also U and ρ were normalized by their upstream values. The form of $A(x)$ shows how lengths are normalized by a scale of the contraction, say l. Thus, in the normalization used in figures 2 and 3, a is now replaced by U_∞/l. Figure 11 shows the prescribed cross-section and Mach number as a function of distance down the contraction, along with the RDT result for the turbulent intensity, $2k$. Figure 12 shows how $\overline{p'^2}$ and $\overline{p'\nabla\cdot\boldsymbol{u}'}$ develop down the nozzle. Far upstream and far downstream the flow becomes uniform, so the rapid distortion pressure vanishes. As the pressure variance rises, the pressure–dilatation correlation becomes negative; farther downstream the pressure variance begins to fall and the pressure–dilatation crosses zero and becomes positive. This behaviour is analogous to that seen in turbulent flow through a shock wave: in that case the pressure–dilatation stores kinetic energy during the compression, then releases it after the shock.

Appendix B. Equations of the turbulence model

The turbulence closure model is presented here only for the case of one-dimensional compression. A general formulation is described in Zerman (1990, 1991), to which the present rapid pressure–dilatation model has been added. Time, τ, is non-dimensionalized by minus the initial rate of compression, $-a_1$, so $S_{11} = -1/(1-\tau)$. Turbulent intensities are normalized by the initial turbulent energy, k_0, and the lengthscale is normalized by $k_0^{\frac{1}{2}}/a_1$. It is convenient to introduce the new dependent variables:

$$B = \overline{u_1^2} - \tfrac{2}{3}k; \quad Y = k + (\overline{p_s'^2} + \overline{p_a'^2})/2\rho^2c^2; \quad R = \overline{p_a'^2}/\rho^2c^2, \tag{B 1}$$

all of which are made non-dimensional by k_0. Y is the sum of the kinetic energy and the potential energy of the pressure fluctuations. In terms of these variables the model equations are

$$\left.\begin{aligned} \dot{B} &= \frac{4(B+\frac{2}{3}k)}{3(1-\tau)} - \Pi_{11}, \quad \dot{Y} = \frac{B+\frac{2}{3}k}{1-\tau} + \frac{\gamma-1}{1-\tau}(Y-k) - \epsilon, \quad \dot{\epsilon} = \left[\frac{B+\frac{2}{3}k}{1-\tau} - 1.84\epsilon\right]\frac{\epsilon}{k}, \\ \dot{L} &= \left[\frac{2}{3}\left(\frac{\epsilon}{(2k)^{\frac{3}{2}}L}\right)^{\frac{1}{2}} - \frac{1}{1-\tau}\right]L, \quad \dot{R} = \frac{R_e - R}{0.2M_T T} - \frac{1-3\gamma}{6(1-\tau)}R, \end{aligned}\right\} \tag{B 2}$$

where $T^2 = (2k)^{\frac{1}{2}}L/\epsilon$, $R_e = 2kM_T^2/(1+M_T^2)$ and $M_T^2 = 2k/c^2$. The pressure–strain model is

$$\Pi_{11} = [3.25/T + 0.6/(1-\tau)]B + 0.4k/(1-\tau).$$

The constants 0.6 and 0.4 in the rapid terms are smaller than in Zeman (1990): his values are 0.8 and 0.53. Their ratio was kept equal to $\frac{2}{3}$. The smaller values were needed to obtain the right level of anisotropy. It should be emphasized that the anisotropy is not sensitive to the pressure–dilatation model, while it is sensitive to the pressure–strain model. It is conceivable that the pressure–strain model requires modification for compressibility effects. The ϵ-equation contains a term which Coleman & Mansour (1991) found necessary to account for the effect of variable viscosity, which is why the constants seem to differ from values for incompressible flow. In the present computation of rapidly compressed turbulence dissipation is largely irrelevant.

The rapid, solenoidal pressure variance model (40) reduces in the present case to

$$\frac{\overline{p_s'^2}}{\rho^2c^2} = \frac{L^2M_T^2}{3(1-\tau)^2}\left(\tfrac{2}{3}C_1 + \frac{C_2B}{2k}\right). \tag{B 3}$$

The RDT values $C_1 = \frac{6}{5}$ and $C_2 = \frac{18}{7}$ were used. Equation (B 3) along with the solution to (B 2) for Y and R determine k. The equation for Y was derived from (7) and the turbulent kinetic energy equation:

$$\dot{k} = -\overline{u_1^2}\,\partial_1 U_1 + \Pi_{\mathrm{d}} - \epsilon.$$

For this purpose, it should be noted that (7) divided by ρ can be rewritten

$$\Pi_{\mathrm{d}} = -\frac{1}{2}\frac{\mathrm{d}}{\mathrm{d}t}\left(\frac{\overline{p'^2}}{\rho^2 c^2}\right) - \frac{(\gamma-1)\overline{p'^2}}{2\rho^2 c^2}\nabla\cdot\boldsymbol{U} \tag{B 4}$$

when the mean flow is isentropic.

REFERENCES

Batchelor, G. K. & Proudman, I. 1954 The effect of rapid distortion on a fluid in turbulent motion. *Q. J. Mech. Appl. Maths* **7**, 83–103.

Bender, C. M. & Orszag, S. A. 1978 *Advanced Mathematical Methods for Scientists and Engineers*. McGraw-Hill.

Blaisdell, G. A., Mansour, N. N. & Reynolds, W. C. 1991 Numerical simulations of compressible homogeneous turbulence. *Rep.* TF-50. Thermosciences Div., Mechanical Engineering Dept., Stanford University.

Coleman, G. N. & Mansour, N. N. 1991 Simulation and modeling of homogeneous compressible turbulence under isotropic mean compression. *8th Symp. on Turbulent Shear Flows, Munich*.

Durbin, P. A. 1981 Distorted turbulence in axisymmetric flow. *Q. J. Mech. Appl. Maths* **34**, 489–500.

Durbin, P. A. & Hunt, J. C. R. 1980 On surface pressure fluctuations beneath turbulent flow round bluff bodies. *J. Fluid Mech.* **100**, 161–184.

Goldstein, M. E. 1978 Unsteady vortical and entropic distortions of potential flows round arbitrary obstacles. *J. Fluid Mech.* **89**, 433–468.

Goldstein, M. E. 1979 Turbulence generated by the interaction of entropy fluctuations with non-uniform mean flows. *J. Fluid Mech.* **93**, 209–224.

Hunt, J. C. R. 1973 A theory of turbulent flow round two-dimensional bluff bodies. *J. Fluid Mech.* **61**, 625–706.

Hunt, J. C. R. & Carruthers, D. J. 1990 Rapid distortion theory and the 'problems' of turbulence. *J. Fluid Mech.* **212**, 497–532.

Launder, B. E., Reece, G. J. & Rodi, W. 1975 Progress in the development of Reynolds stress turbulence closure. *J. Fluid Mech.* **68**, 537–566.

Lee, S., Lele, S. K. & Moin, P. 1991 Direct numerical simulation and analysis of shock turbulence interaction. *AIAA Paper* 91-0523.

Ribner, H. S. & Tucker, M. 1953 Spectrum of turbulence in a contracting stream. *NACA Rep.* 1113.

Sabelnikov, V. A. 1975 Pressure fluctuations generated by uniform distortion of homogeneous turbulence. *Fluid Mech. Soviet Res.* **4**, 46–57.

Wong, W. W. & Hoult, D. P. 1979 Rapid distortion theory applied to turbulent combustion. *SAE Tech. Paper* 790357.

Zeman, O. 1990 Dilatation dissipation: the concept and application in modeling compressible mixing layers. *Phys. Fluids* A **2**, 178–188.

Zeman, O. 1991 Compressible turbulence subjected to shear and rapid compression. In *8th Symp. on Turbulent Shear Flows, Munich*.